Analytica Chimica Acta 1278 (2023) 341711

Contents lists available at ScienceDirect

Analytica Chimica Acta

journal homepage: www.elsevier.com/locate/aca

Fluorescent nanostructured carbon dot-aptasensor for chlorpyrifos detection: Elucidating the interaction mechanism for an environmentally hazardous pollutant

María Isabel Gaviria-Arroyave [a,*], Juan Pablo Arango [b], Kaory Barrientos Urdinola [b], Juan Bernardo Cano [c], Gustavo Antonio Peñuela Mesa [a]

[a] GDCON Research Group, Engineering Faculty, Universidad de Antioquia, Colombia
[b] GIBEC Research Group, Life Sciences Faculty, Universidad EIA, Colombia
[c] GIMEL Research Group. Engineering Faculty, Universidad de Antioquia, Colombia

HIGHLIGHTS

- A biosensor based on ssDNA aptamer and Carbon Dots was developed for CPF detection.
- The mechanism of interaction for the aptamer and CPF was proposed through docking modeling.
- The biosensor shows low LOD for CPF and good specificity.
- The biosensor showed good detection of CPF in superficial waters.

GRAPHICAL ABSTRACT

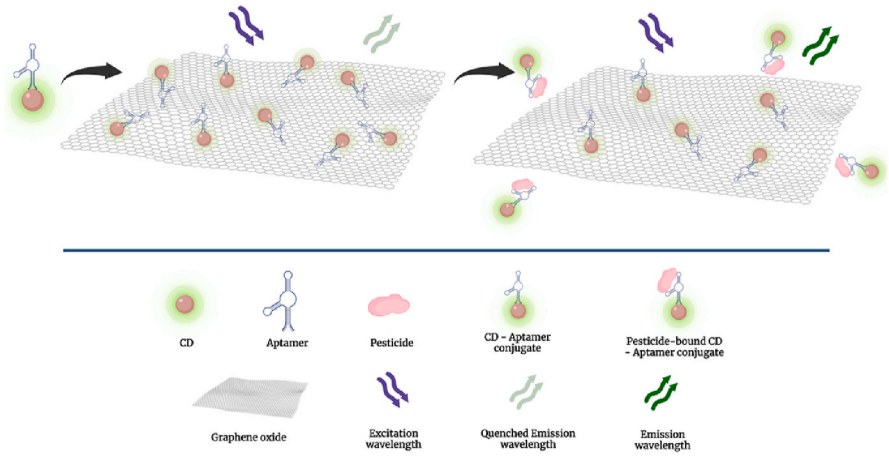

ARTICLE INFO

Handling Editor: Professor Chuck Henry

Keywords:
Aptamers
Chlorpyrifos
Fluorescent biosensor
Carbon dots
Graphene oxide

ABSTRACT

Chlorpyrifos (CPF) is a commonly used insecticide found in many water sources and is related to several health and environmental effects. Biosensors based on aptamers (single-stranded nucleic acid oligonucleotides) are promising alternatives to achieve the detection of CPF and other pesticides in natural waters. However, several challenges need to be addressed to promote the real application of functional aptasensing devices. In this work, an ssDNA aptamer (S1) is combined with carbon quantum dots (CD) and graphene oxide (GO) to produce a stable fluorescent aptasensor characterized through spectrophotometric and electrophoretic techniques. For a deeper understanding of the system, the mechanism of molecular interaction was studied through docking modeling using free bioinformatic tools like HDOCK, showing that the stem-loops and the higher guanine (G) content are crucial for better interaction. The model also suggests the possibility of generating a truncated aptamer to

* Corresponding author.
E-mail address: mariai.gaviria@udea.edu.co (M.I. Gaviria-Arroyave).

https://doi.org/10.1016/j.aca.2023.341711
Received 4 April 2023; Received in revised form 10 August 2023; Accepted 11 August 2023
Available online 12 August 2023

improve the binding affinity. The biosensor was evaluated for CPF detection, showing a low LOD of 0.01 μg L^{-1} and good specificity in tap water, even compared to other organophosphates pesticides (OPs) like profenofos. Finally, the recovery of the proposed aptasensor was evaluated in some natural water using spiked samples and compared with UPLC MS-MS chromatography as the gold standard, showing a good recovery above 2.85 nM and evidencing the need of protecting ssDNA aptamers from an erratic interaction with the aromatic groups of dissolved organic matter (humic substances). This work paves the way for a better aptasensors design and the on-site implementation of novel devices for environmental monitoring.

1. Introduction

The agricultural value chain has been heavily reliant on pesticides for almost 60 years. According to the Food and Agriculture Organization (FAO) in 2018, the world consumption of pesticides reached 4 million tons and by 2020, the top 5 countries with the highest annual consumption (data in thousands of tons) were the United States (407), Brazil (377), China (262), Argentina (245), and the Russian Federation (90) [1]. Pesticides can be absorbed by people in a variety of ways. For instance, agriculture workers in developing countries like Colombia could be exposed to pesticides by crop use and because of the runoff processes to water as well. Pesticide exposure has been linked to major illnesses like non-Hodgkin lymphoma [2], Parkinson's disease [3] as well as respiratory and reproductive disorders [4]. According to estimates, more than 300,000 people died because of pesticide poisoning [5].

Organophosphate pesticides (OPs) are the widest group of insecticides used worldwide. OPs cause neurotoxicity because they can irreversibly inhibit the acetylcholinesterase enzyme (AChE) in the nervous system [6]. Chlorpyrifos (CPF), one of the OPs, is the primary active ingredient used in many crops and has a relatively low persistence. However, typical bioactive compounds like CPF and CPF-oxon block AChE. Despite its ban in 2021 by EPA, CPF is still being used in developing nations under the brand names Lorsban, Dursban, Equity, Suscon, Empire 20, and Whitmire PT27 [7].

For the detection of OPs, some high-precision analytical technologies have been used, including gas chromatography (GC), high-performance liquid chromatography (HPLC), and mass spectrometry (MS) [8]. However, some drawbacks like complicated operation, high cost, and lengthy-time consumption, evidence an urgent need for the development of a simple, quick, and stable detection technology for OPs. Especially for on-site monitoring.

In this scenario, biosensors have emerged as viable instruments for quick and accurate OPs detection. More stable optical biosensors based on nanomaterials have been created recently, achieving lower detection limits [7, 9, 10]. The application of nanomaterials, including Carbon Quantum Dots (CD), can significantly improve the performance of the systems [11,12]. CD are carbonaceous nanomaterials with sizes less than 10 nm. CDs are non-toxic and they benefit from all the Quantum dots' advantages, including spectral tunability of the emission spectrum and resistance to photo-bleaching [13]. Due to their natural fluorescence, CDs have attracted a lot of attention [14]. Even though CD increase sensitivity, the use of biomolecules with higher specificity must be considered to promote the commercial application of biosensors.

Aptamers are short single-stranded oligonucleotides (RNA or DNA) developed through the Systematic Evolution of Ligands by the Exponential Enrichment method (SELEX), which can selectively bind to their targets with high affinity [5]. Aptamers have recently drawn a lot of interest as recognition components for a variety of targets, including small compounds, proteins, and pesticides [5]. Aptamers have several benefits over enzymes and antibodies commonly used for OPs detection, including higher thermostability, protease resistance, cost-effectiveness, in vitro production, minimum batch-batch variation, small size, simplicity of modification, and target flexibility [15]. Aptameric technology is still in an early stage of development, especially in the environmental field. The main technical problem in developing aptamers for OPs recognition is the small molecular structure of the targets, limiting the interactions between their functional groups and aptamer sequences and making the SELEX process quite complex. Only roughly 20 established pesticide targets have aptamers after 30 years of development; CPF is among those pesticides [15].

Different nanomaterial-based optical aptasensors have been developed in the last few years for pesticide detection. The use of colorimetric, fluorescent, surface plasmon resonance, SERS, and chemiluminescent methods for the detection of several types of pesticides besides OPs has been reported [16]. Fluorescent aptasensors have been used preferably over other kinds of biosensors because of their high sensitivity and, some fluorescent transductors have been used for ultra-sensible detection in picomolar ranges. For example, Cu nanoparticles (CuNPs) for Isocarbophos [17]; sulfur-doped graphene Quantum dots for the sensing of Omethoate [18], and bimetallic metal–organic frameworks (MOF) for Acetamiprid quantification [19]. Those results are outstanding in terms of sensibility and specificity but the complexity in the construction using multiple aptamers and nanomaterials could limit the on-field application. Moreover, for environmental monitoring, the use of more sustainable nanomaterials like CD is a must.

The mechanism for OPs and other small molecule detection using nanostructured aptasensors is related to the so-called Förster resonance energy transfer (FRET); also referred to as fluorescence resonance energy transfer [13]. FRET is a non-radiative energy transfer process that typically takes place between two fluorophores (or a fluorophore and a quencher) at about 10 nm (Förster distance), where an emitter is close to an acceptor and transfers energy from an excited state through dipole-dipole interactions [20]. This interaction is reflected in an overlap of absorbance-emission spectra. Graphene oxide (GO) is an excellent quenching agent because of its high efficiency and broad absorption spectrum. GO is an innovative nanomaterial made of a two-dimensional graphitic carbon structure that is only one atom thick. Additionally, it has many functional groups with oxygen on the surface, including carboxyl, hydroxyl, and epoxy groups. Because of the carbonaceous skeleton of GO, single-stranded oligonucleotides can be absorbed through hydrophobic and π stacking interactions, thus quenching the fluorescence of the CD by FRET [21].

In this work, we integrate the fluorescent properties of CD with a ssDNA aptamer, and the quenching properties of GO, to develop a biosensor for CPF detection in water samples. To get deeper into the detection mechanism, we use bioinformatic tools for modeling the CPF-aptamer interaction. An understanding of the tertiary structure of aptamers is crucial to promote better interactions with the targets. For this purpose, in silico methods have been used including aptamer-target docking models and computational tools to predict aptamer structures and thermodynamic properties. Thus, they might enable the modification of a specific set of nucleotides to enhance aptamer performance, saving experimental time compared to the traditional trial-and-error method [22]. This methodology could be applied for future aptasensor simulations under key conditions like [Na+], pH, or temperature, thus leading to an optimizing system.

Finally, we evaluated the biosensor for the detection of CPF in superficial water samples from different sites in Antioquia, Colombia. The results showed that the developed aptasensor is a promising alternative for the detection of CPF. However, further research must be carried out

to improve the specificity and reduce the interference of the system by organic matter. This work paves the way for optimization steps in the aptamer's design and application as fluorescent probes.

2. Materials and methods

2.1. Chemicals and reagents

Aptamer S1 [23, 24] was synthesized by Eurogentec® with the characteristics presented in Table 1. S1 was prepared at 32.24 μM using double-filtered (0.2 μm) PBS (1 X) and keep it at −20 °C until use. A terminal amine modification (5' Amino modifier C6) was included to use the carbodiimide conjugation technique as a covalent bond to CD. All chemicals were analytical grade. An analytical standard of Chlorpyrifos (CPF) and PBS tablets were bought from Merck. Carbon dots (CD) were synthesized pyrolytically from African oil palm biochar (*Elaeis guineensis*) according to our previous work [25]. For conjugation steps, EDC (1-ethyl-3-[3-dimethylaminopropyl] carbodiimide), NHS (N-hydroxysuccinimide), and 2-mercaptoethanol (ME) were bought from Thermo Fisher. Single-layered graphene oxide (GO) was purchased from ACS material. All tests were carried out in triplicates. Double deionized water was used throughout all the experiments (Milli-Q ultrapure water system with a 0.22 μm filter, Merck Millipore).

2.2. Conjugation procedure

The covalent conjugation technique was used through carbodiimide chemistry following the protocol described in our previous work [7] with some modifications. Briefly, 500 mg L^{-1} of CD water solution was put in contact with 0.05 M of EDC and 0.1 M of NHS and let them react for 15 min followed by 2 h dialysis (3.5 kDa, 4 water changes). Before the addition of S1, the pH was adjusted to 7.45 with sodium bicarbonate and an optimized NaCl concentration of 0.137 M was adjusted by using PBS tablets. An appropriate amount of S1 (final concentration of 1 μM) was added and left reacting for 4 h at 25 °C and 50 rpm. The S1 conjugate was left overnight at 4 °C followed by 30 min of dialysis (3.5 kDa, 2 water changes). The S1 conjugates were stored under 4 °C until detection assays and remained active for at least 1 week.

2.3. Instrumentation

UV–Vis and fluorescence measurements (spectrum and punctual) were done in a Varioskan Lux (Thermo scientific, SkanIt Software 4.1) on a 200 μL working volume microplates (Falcon™ non-treated black 96-well) at 25 °C with 1 nm optical step. To verify the conjugation between aptamer and CD, agarose gel electrophoresis was used in 6.0% agarose gel with 0.5 × TBE buffer at 100 V for 1 h. For the verification of the recovery in spiked samples, UPLC MS-MS chromatography was used as standard gold (Water manufacturer; Xevo TqD, UPLC-HClass; serial MS QCA032; pump F11QSM343A; Injector F11SDI5616).

2.4. Molecular simulation

For a better understanding of the interaction mechanism between S1 and CPF, some free bioinformatic tools were applied as described in Fig. 1, based on the proposal by Oliveira and collaborators [22]. Briefly, using the S1 sequence, the 5 most probable secondary structures were generated with the Mfold web server, considering the most stable configuration (minimization of the free energy) [26]. Each secondary structure was refined with PyMOL software by adding the hydrogens that are usually omitted in the Mfold prediction since those hydrogens play a major role in aptamer's interaction with targets [27]. Before the docking simulation, the CPF tertiary structure (CID 2730) was obtained from the PubChem database [28] in SDF format followed by a cleaning step and hydrogen addition with PyMOL. Both S1 and CPF tertiary structures were saved in PDB format. Finally, for the elucidation of the interaction mechanism the docking models were evaluated by each combination of S1 – CPF tertiary structures using the free HDOCK web server [29]. The model with the lowest docking score (more possible binding model) was selected.

2.5. Pesticide detection

CPF was evaluated in a range between 0 and 0.1 mg L^{-1}. For this purpose, different dilutions were made in Milli-Q water from a stock solution of 100 mg L^{-1} preserved in methanol. For the detection assay, 440 μL of the conjugate and 10 μL of GO (100 mg L^{-1} GO final optimized concentration) were vigorously mixed in different vials. After 30 min at 50 rpm, 50 μL of the appropriate dilution of the pesticide were added to reach the desired final concentration. The solution was vigorously mixed and incubated for 1 h (optimized time) until fluorescence recovery analysis. The amount of the pesticide dilution was replaced by Milli-Q water for control. The fluorescence intensity (recovery) at emission and excitation wavelengths of 420 and 320 nm (respectively) was recorded and plotted against the CPF concentrations (higher recovery means higher CPF concentration). For the estimation of the limits of detection (LOD) and quantification (LOQ), a semilog plot in the linear range was generated and the parameters of the curve were used to estimate LOD as the concentration corresponding to the mean blank value plus 3 times the standard deviation (SD) of the blank [30]. The LOQ was defined in the same way, considering a 10 times parameter. All experiments were treated and analyzed in triplicate. For LOD calculations, a one-way ANOVA was performed using R-studio software, and $p \leq 0.05$ was considered statistically significant.

2.6. Pesticide detection in superficial water

Superficial water samples were taken from 3 different locations in the department of Antioquia, Colombia. Some physicochemical parameters of the samples were evaluated (pH, COD, electric conductivity, and true color), as they can be influential variables in the detection assay. Even though the water samples were taken from some rural locations with previous reports of pesticide pollution by run-off water, the UPLC/MS evaluation showed no CPF detection. Considering this, the samples were used as an actual matrix for the experimental procedure of spiked samples. For each sample, 3 CPF concentrations were used (0.1, 1 y 10 μg L^{-1}) and the recovery of the aptasensor was compared to UPHLC/MS as the gold standard. All experiments were treated and analyzed in triplicate and the %RSD parameter was estimated.

Table 1
ssDNA aptamer (S1) characteristics.

Sequence	5-CCTGCCACGCTCCGCAAGCTTAGGGTTACGCCTGCAGCGATTCTTGATCGCGCTGCTGGTAATCCTTCTTTAAGCTTGGCACCCGCATCGT- 3
Length	91 pb
Modifications	5′ Amino Modifier C6
Purification	PAGE
Scale	10 μmol
Melting point	75.9 °C
Molecular weight	28025.2 g/mol

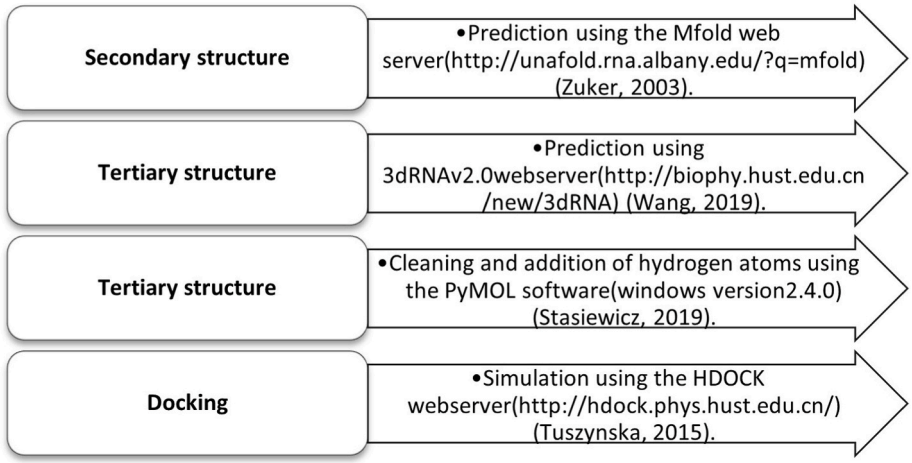

Fig. 1. Workflow for the in-silico simulation of the S1-CPF interaction, showing the expected results on the left and the methods and tools on the right. Free bioinformatic tools like Mfold, #dRNAv2, and HDOCK were used. Modified from [22].

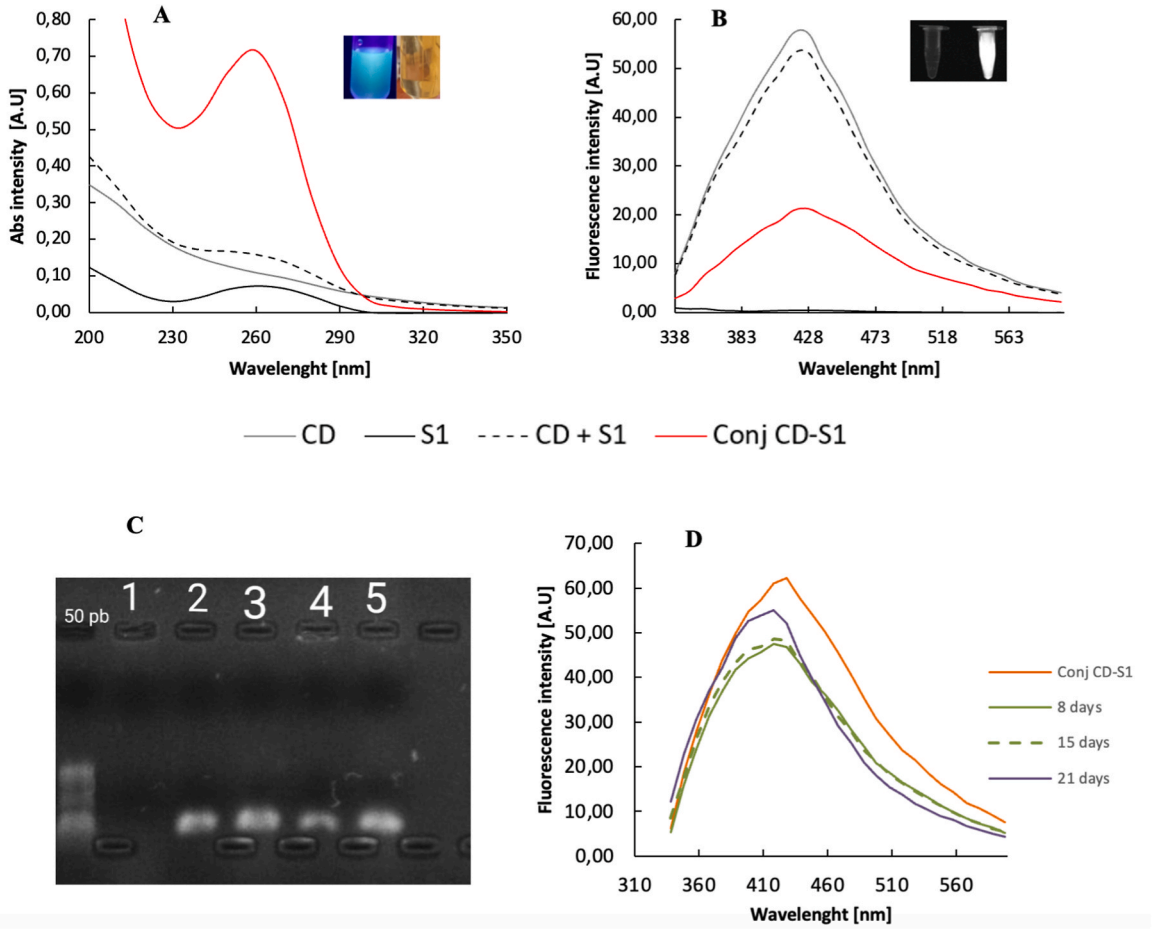

Fig. 2. A) UV–Vis spectrum showing the increase of the peak at 260 nm for the conjugated CD and S1 at 1 μM, due to the amide bond formation thus confirming the conjugation process. B) fluorescence emission spectrum (Excitation at 320 nm) showing the decreasing of the fluorescence of the CD for the conjugation of CD and S1 at 1 μM because of the surface chemistry modification. The inserts show the CD under UV light and the mili Q water control. C) showing conjugate CD-S1 (line 2) moving slower than bare S1 (line 3) thus confirming the presence of a heavy molecule because of the conjugation process. D) showing the stability follow-up of the conjugate to 21 days, presenting a decrease in the fluorescence signal at 8 days due to aggregation phenomena followed by a fluorescence recovery related to the hydrolysis of the covalent bond and suggesting the use of fresh conjugate for the detection assays.

3. Results and discussion

3.1. Conjugate characterization

CDs were synthesized pyrolytically from African oil palm (*Elaeis guineensis*) and characterized in our previous work [25]. CD have plenty of carboxylic groups and they had a maximum emission peak at $\lambda = 420$ nm under excitation of $\lambda = 320$ nm. CD have a brownish-yellow color under daylight and blue emission under ultraviolet light (insert in Fig. 2A). To demonstrate superficial modification of the CD by a covalent conjugation with S1 (amide bond formation), UV–Vis and fluorescence spectra were evaluated, as well as agarose gel electrophoresis. The UV–Vis spectrum in Fig. 2A showed the CD with an absorption peak of 260 nm, in agreement with our previous work reported the peak for the CD of *Elaeis guineensis* between 260 y 280 nm possibly attributable to n-π* transition of C=O bonds [25]. In the same figure, the spectrum for the simple mix of CD and S1 (without conjugation) and the conjugate CD-S1 are shown, evidencing a remarkable peak at 260 nm for the conjugate. Since both, the simple mix and the conjugate have the same amount of CD and S1, the increase of the peak at 260 nm in the conjugate could be attributable to amide-bond formation between the amino C6 modifier at the 5' termini of the aptamer and the free carboxylic acids in the CD. In fluorescent probes based on nanomaterials and aptamers, usually, peaks between 260 and 280 nm are found [31]. Also, is known that DNA aptamers like S1 have an absorption peak at 260 nm [32]. Regarding the fluorescence spectrum shown in Fig. 2B, for all the samples, a maximum emission peak was obtained at 420 nm with 320 nm as the excitation value. We can see in the fluorescence spectrum, how the conjugated mixture decreases the original fluorescence of the CD, because of the modification of the surface chemical groups in the CD; this mechanism is directly responsible for the fluorescence behavior [14]. Although the fluorescence peak remains around 428 nm for all the samples, the conjugate showed a slight red shift from 418 nm to 428 nm. Different authors have reported this behavior as evidence of conjugation [21, 33, 32].

Fig. 2C shows that the conjugate CD-S1 moves slower than the bare S1 (lines 2 and 3 respectively) due to the increase in the mass-to-charge ratio in the conjugate [21]. Lines 4 and 5 correspond to another aptamer-CD combination not used in this work. Finally, a following in the stability of the conjugate stored at 4 °C was done. Fig. 2D shows the characteristic fluorescence emission peak at 428 nm for the fresh conjugate. After 8 days, the fluorescence of the conjugate decreased by 24% probably due to aggregate formation, and a blue shift to 418 nm appeared. The same behavior could be observed after 15 days. However, after 21 days, the fluorescence intensity grew, and the blue shift was encouraged. This increase in the fluorescence intensity has been observed in our previous work [7], and together with the blue shift, is evidence of the loss of the covalent amide bond, thus showing a trend to a recovery of the bare CD fluorescence intensity. Those results evidence the successful conjugation of the CD-S1 and suggest the priority use of the fresh conjugate for the detection experiments.

3.2. Molecular interaction and docking model

The detection mechanism of the proposed sensor is shown in Fig. 3. CD are covalently bonded to S1 causing a decrease in the fluorescence intensity. Then we added an optimized GO concentration of 100 mg L^{-1}, reducing to 63% the initial fluorescence and indicating the quenching phenomena (FRET) in a turned-off system. GO is reported as a highly efficient quencher, especially when it's used with aptamers since mRNA and ssDNA are absorbed in GO through π interactions using their organic nitrogenous bases [13]. When the pesticide molecules are present, the molecules interact with the aptamers and the desorption happened due to structural changes in the aptamers since there are highly selective to their targets. This mechanism (turn-on mode) has been reported by several authors [21, 34, 35].

For the docking model, a general workflow illustration is presented in Fig. 4. Starting only with the aptamer sequence presented in Table 1, the secondary structure of the aptamer in the lowest energy state was predicted with a Gibbs free energy (G) of −15.47 kcal mol^{-1} at 37 °C to explore the binding of S1 aptamer to CPF (Fig. 5A). A greater negative ΔG value results in a more stable aptamer-target complex and it depends on the relationship between the enthalpy, and entropy changes (ΔH, and ΔS respectively) at a given temperature ($\Delta G = \Delta H - T \cdot \Delta S$) [36]. For the secondary structure of S1, we found −182.3 kcal mol^{-1} and -0.537.9 kcal $(K\ mol)^{-1}$ for ΔH and ΔS respectively. The negative enthalpy value implies an increased number of interactions between the aptamer and the target, but this parameter also considers the solvent interactions. The

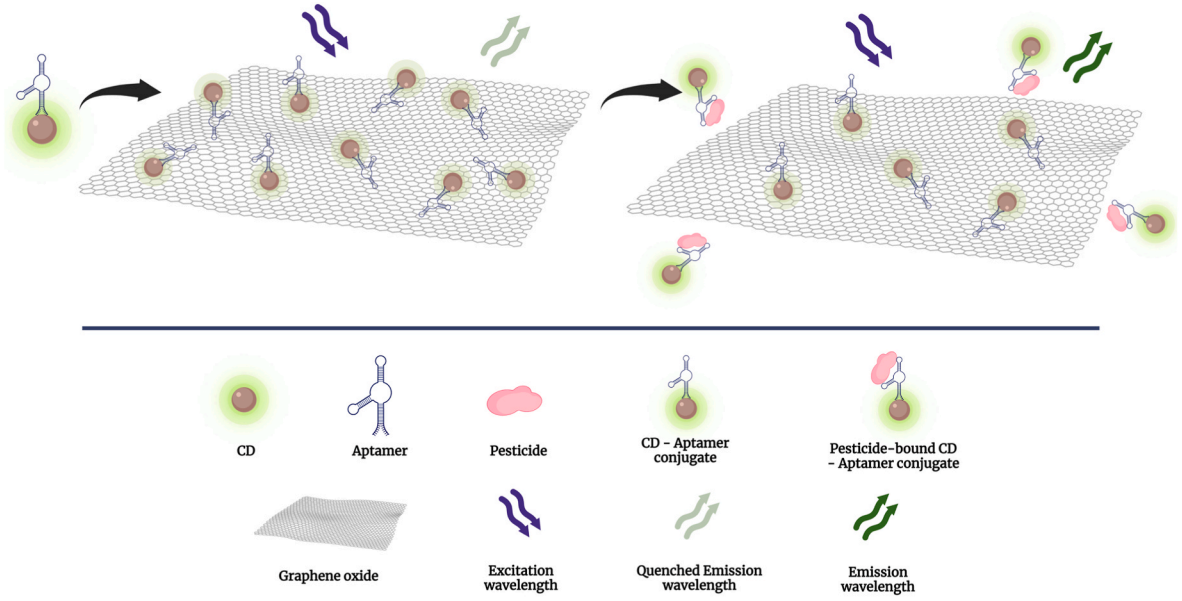

Fig. 3. The detection mechanism of the proposed sensor. The conjugate molecules between CD and S1 aptamer are attracted by the GO through aromatic stacking forces (π-π), enabling the quenching effect because of the FRET phenomena. Then, in the presence of CPF, the stronger attraction with the aptamer generates the conjugate molecules to detach from the GO, thus recovering the fluorescence signal proportionally to the CPF concentration.

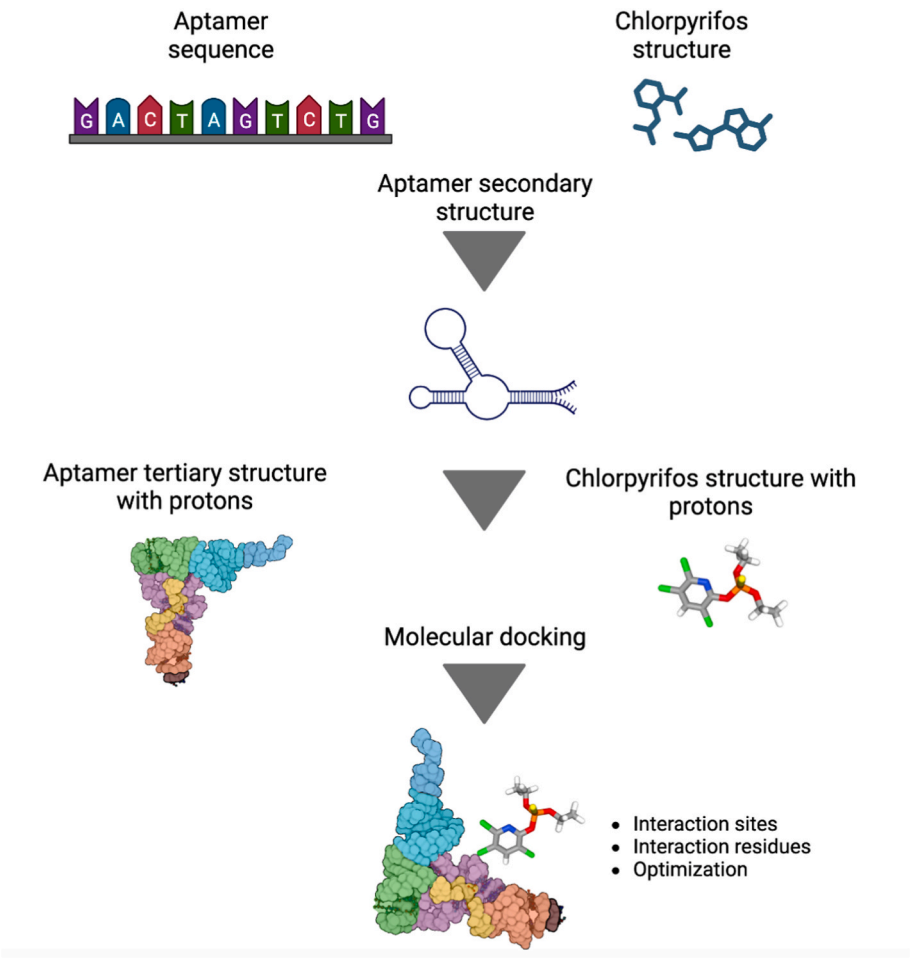

Fig. 4. Illustration of the general workflow of molecular docking calculations. The process starts with a sequence, then secondary and tertiary structures are obtained including protonation. Finally, a blind docking simulation is performed generating a ranked list of possible complexes between aptamer and pesticide.

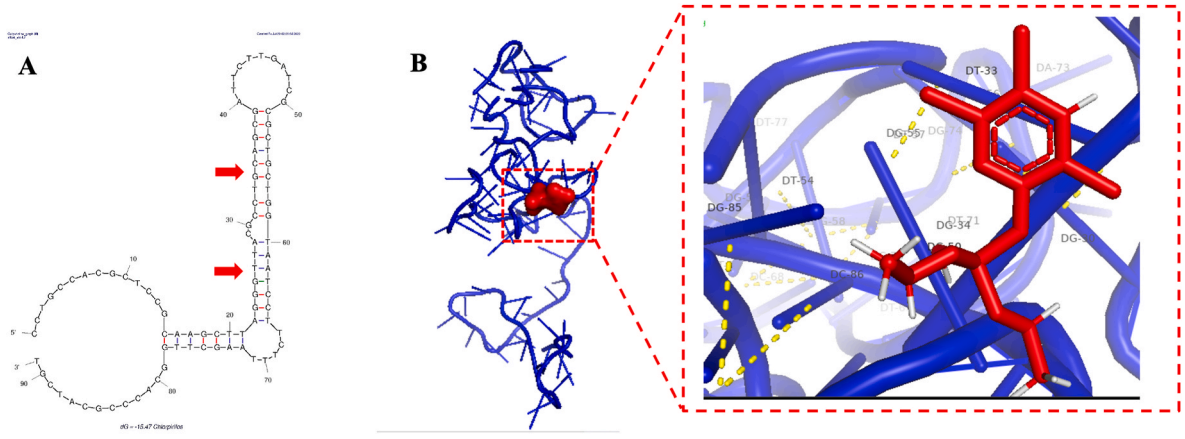

Fig. 5. Results of the molecular interaction of chlorpyrifos with S1 aptamer. A) secondary structure indicating the most probable interaction sites probably associated with G-quadruplexes. B) 3D structure showing the interaction site with the lower docking score. Insert zoom of the interaction site in B showing the corresponding residues and the aromatic stacking (π- π) interactions like yellow dotted lines.

entropy value could be related to the loss of the rotation and translation degrees of freedom of the aptamer-target complex compared to the free molecules. The results suggest that S1-CPF interactions are driven by enthalpy-entropy compensation since both parameters have favorable contributions [36]. The secondary structure (Fig. 5A) also has a higher content of G (24%) compared to the other generated structures. A more stable nucleic acid sequence is made possible by this structural feature and the G content is also known by generating G quadruplets, crucial areas, and binding sites [37]. The S1 secondary structure exhibits stem-loops and internal loops that could undergo conformational changes by stacking forces and electrostatic interactions leading to specific recognition areas for CPF.

With the secondary structure, five probable tertiary structures were generated. For each tertiary structure, the binding model to CPF was

conducted using the molecular docking technique in the HDOCK web-server. The model with the lowest docking score (more probable binding site) is represented in Fig. 5B and suggests that the CPF molecule is embedded in the S1 pocket. The main binding sites (distances below 5 Å) are T33, G34, T48, G50, C51, G87, C86, A87, and T88. Those residues are pointed out in the secondary structure and evidence of the importance of G content and the loops. The CPF molecules connect to the stem-loop region of S1 through conjugation interactions, and these interactions are crucial for the stable binding of both CPF molecules and the aptamer [37]. The most common interaction forces in the detection of OPs through aptamers have been described as, the C–H bond, π-π interactions, and H-bond interactions [38]. For the S1-CPF model, the results show that the interactions are primary π-π, thus some modifications could be proposed to obtain stronger forces like H-bonds. This is important considering that S1-GO interactions are also π-π stacking, but a better detection implies a stronger attraction force between S1 and CPF than the S1 and GO. For instance, it seems like the pocket is not blocked by the CD conjugation, since the model shows a good distance between the conjugation site (5') and the pocket. Future works should use advanced bioinformatic tools like the PLIP web server [39] for the identification of specific chemical groups related to the interactions with small molecules.

To improve the interaction between S1 and CPF, the size of the stem-loop can be changed, and mutations can be made to better fit the desired range of analyte concentration. Given the high amount of guanine in S1, it is important to carefully examine the mechanism of G-quadruplexes. Regarding the results of the 3D model, it could be inferred that a smaller or truncated aptamer could be generated to obtain a better docking score and more stable interactions. Moreover, there are a few reports about the molecular interaction between aptamers and OPs targets, so these findings represent an important contribution to the current state of the art.

3.3. Quantification of CPF

Different CPF concentrations (0–0.1 mg L^{-1}) were examined. Fig. 6A shows the rise in fluorescence response for CPF detection as a function of pesticide concentration. Despite the differences in the fluorescence signal at the concentration range being low, a good exponential correlation between fluorescence intensity and CPF concentration is shown in Fig. 6B. Moreover, Fig. 6C shows a good linear relationship of fluorescence with the natural logarithm of CPF concentration between 0 and 7.5 μg L^{-1} (0–21.6 nM). The linear regression equation for this range (R2 = 0.9907, $***p < 0.001$, $n = 3$) was F = 25.45 + 0.3122 Ln C, where F and C are the fluorescence intensity and CPF concentration, respectively. The LOD and LOQ were calculated as low as 0.01 μg L^{-1} (0.028 nM) and 0.1 μg L^{-1} (0.28 nM) respectively. This is consistent with the detection mechanism previously described, according to which the more CPF present in the system, the more CD-S1 conjugates detached from GO sheets, resulting in an increase in distance and the inability to perform FRET, which results in the fluorescence recovery of the CD. However, some strategies mentioned in the previous section Molecular interaction and docking model should be applied in future works to improve the overall performance of the proposed aptasensor.

The relative standard deviations (RSD) of the measurements showed a maximum value of 4.15% so the repeatability of the system can be considered as good compared to the state of the art [16].

The LOD of the proposed fluorescent probe based on CD-S1 and GO was compared with other aptasensors for OPs detection in Table 2. The LOD of this work is like or even lower than other sophisticated methods but uses simple strategies and nanomaterials. This work uses a non-doped CD and a simple well-established quencher (GO), obtaining a

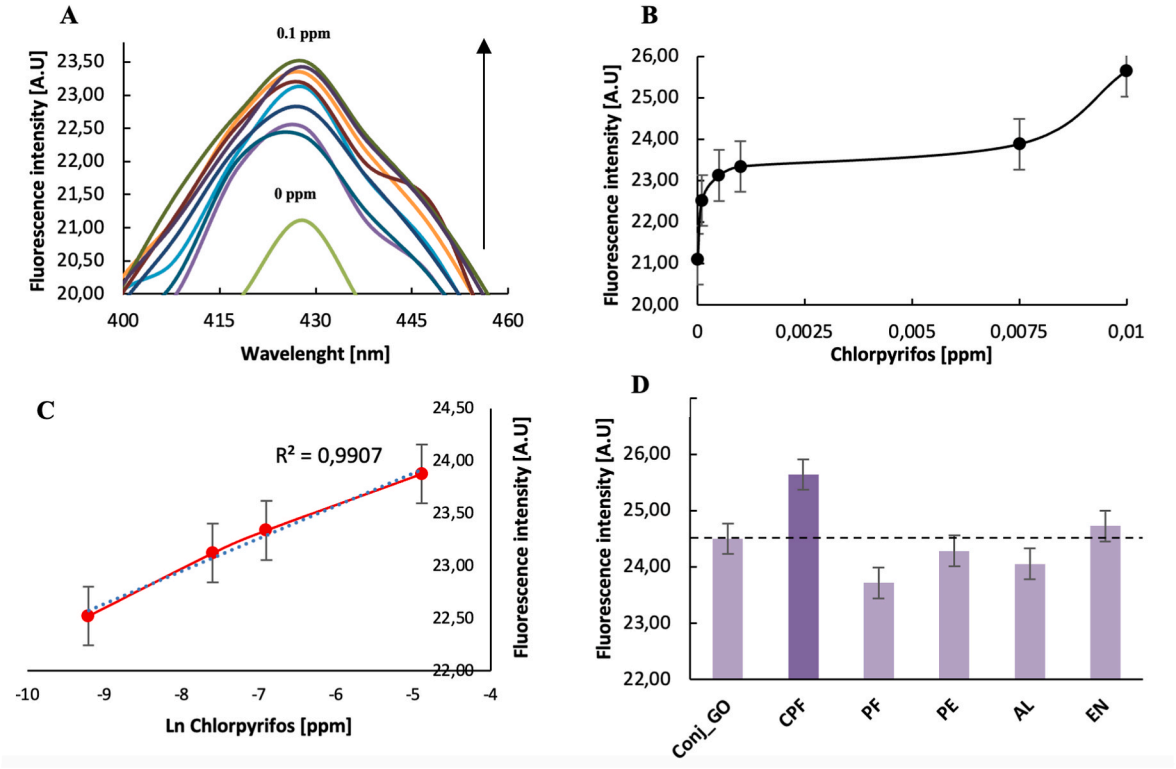

Fig. 6. A) Emission spectra for Chlorpyrifos between 0 and 0.1 μg L^{-1} showing the recovery of the fluorescence signal proportional to the CPF concentration. B) Exponential relationship between the Fluorescence intensity (λem = 420 nm) and the concentration of chlorpyrifos. C) Linear relationship between the Fluorescence intensity (λem = 420 nm) and the natural logarithmic value of chlorpyrifos concentration as a model to obtain the parameters for the LOD calculation. D) Specificity of the system for individual tests of chlorpyrifos (CPF), profenofos (PF), permethrin (PE), aldicarb (AL) and endosulfan (EN). Interference factors at 0.025 μg L^{-1} and CPF at 0.01 μg L^{-1}. The results in D show the good specificity of the system even for the quantification of CPF in the presence of other OPs like PF. The dotted line indicates the baseline (CD-S1 conjugate with GO). n = 3 independent experiments.

Table 2
Comparison of the present method with other reported aptasensors for OP detection shows this work has a sensible LOD compared to other complex systems.

Detection method	Nanomaterial	Aptamer type	Pesticide	LOD (μg L^{-1})	Ref
Fluorescence	None	Tetramethylrhodamine (TAMRA)-labeled aptamer and cDNA.	Phorate Profenofos Isocarbophos Omethoate	0.333 0.167 0.267 0.333	[41]
Fluorescence	Gold nanoparticle. MOF	ssDNA	Chlorpyrifos	1.33	[42]
Fluorescence	L-cysteine capped ZnS quantum dot and GO	ssDNA	Edifenphos	0.1	[40]
Fluorescence	GO	ssDNA	Acephate	4	[34]
Microcantilever- optical	None	ssDNA	Profenofos	1.3	[43]
Ratiometric-electrochemical	carbon nanohorns/Au nanoparticles	Hairpin DNA	Malathion Omethoate	0.013 0.028	[44]
Electrochemical	Complexes of GO and polyaniline (GO@PANI). Gold nanoparticles	ssDNA	Profenofos	0.105	[45]
Electrochemical	Ag@Au nanoflowers	ssDNA	Prometryn	0.06	[46]
Electrochemical	Core–shell nanoparticles Ag@Au NPs and Cu2O@Au NP	Complementary ssDNA	Acetamiprid Malathion	0.043 0.063	[47]
Colorimetric	MOF. Fe–Co magnetic nanoparticles. Fe–N–C nanozymes	Carboxyl functionalized aptamer and cDNA	Phorate Profenofos Isocarbophos Omethoate	0.16 0.16 0.03 1.6	[48]
Colorimetric	Octahedral Ag_2O nanoparticles	ssDNA	Carbendazim	7.35	[49]
Fluorescence	Carbon dots and GO	ssDNA	Chlorpyrifos	0.01	This work

sensitive LOD with a simple and reproducible methodology. However, the narrow linear range of the system should be improved for field application.

Regarding specificity, different pesticides were evaluated at 0.025 μg L^{-1} in the presence of 0.01 μg L^{-1} of CPF. Analogs of CPF or jointly applied insecticides were selected for the study. The results (Fig. 6D) show that the system is specific since the response to CPF is remarkable compared to the other class of pesticides (other organophosphates, pyrethroid, carbamate, organochlorine). The fact that the system did not detect profenofos is important since most of the enzymatic systems commonly used for OPs detection cannot differentiate between CPF and PF structures. Those systems are also interfered with by pyrethroid compounds like permethrin [7]. The small signal to endosulfan (organochlorine) has been reported previously in other aptameric systems for OPs (Arvand and Mirroshandel, 2017). These findings demonstrated that the CD-S1/GO ensemble assay had good specificity toward CPF, which may be attributable to the aptamer's high affinity toward CPF via the FRET system. However, some pretreatment steps could be considered to increase specificity and amplify the output signal.

Finally, to investigate the reproducibility of the system, four aptasensors were prepared in different batches and tested against 0.01 mg L^{-1} of CPF with an RSD value of 3.59%, indicating that the designed aptasensor in this study was reproducible.

3.4. CPF recovery in real water samples

All the samples related in Table 3 showed no signal for CPF by UHPLC/MS, so they were used as an actual matrix for spiked-recovery assay using three different CPF concentrations. The results shown in Table 4 are closely correlated with some physicochemical parameters of the samples (Table 3). For the samples of Santa Elena and San Cristóbal localities spiked with 1 or 10 μg L^{-1}, the recovery rates were found between 84.3% and 125.13% with a maximum %RSD value of 6.75%. Those values agree with the UHPLC recoveries and confirm the potential of the method. However, the samples of the same localities with the lowest amount of CPF (0.5 μg L^{-1}) did not show any signal, suggesting a stronger interference effect for the lowest amount of pesticide and confirming the need for optimization of the aptamer structure.

The spiked samples of the Rio Grande reservoir did not show any recovery signal with the proposed method, suggesting that some parameters like low electric conductivity, higher COD, and Color have a strong influence on the performance of the aptasensor. Ionic strength is well known as a critical factor in the design of aptasensors and some works reported the influence of certain salts (KCl, NaCl, $MgCl_2$, Na_2CO_3) when in a concentration above 100 mM [50].

Rio Grande sample had a greenish color and presence of the superficial vegetation. The true color parameter of the water is due to the presence of dissolved organic matter (humic substances) or certain metals such as iron, manganese, or copper. The organic matter is confirmed with a higher value of COD. Some organic components like dissolved humic acid had fluorescence excitation/emission wavelengths that could interfere with the FRET sensing mechanisms [50]. Also, humic substances have been studied because their aromatic groups could interact with ssDNA leading to a partial or total shielding effect. In this sense, a recent work [51] reported that the carboxyl group and aromaticity of the natural organic matter, the presence of cations, and the relative amounts of ssDNA and organic matter in the system are crucial to understanding the interactions. The shielding effect of the organic matter in ssDNA is determined by interactions between the aromatic portions in the organic matter and the exposed nucleobases of ssDNA. Aldrich humic acid showed a higher interference. Regarding the cation bridging effect, Ca^{2+} showed the highest interference (above Mg^{2+}), since when Ca^{2+} is present even a small amount of Aldrich humic acid could completely inhibit the detection by ssDNA aptamers like S1

Table 3
Detailed locations and some physicochemical parameters of the superficial water samples showing Santa Elena and San Cristobal localities with low organic matter (COD and Color) and Rio Grande reservoir with high organic matter content and low electric conductivity.

Sample	Coordinates	Description	pH	Electric conductivity (μS/cm)	COD (mg O_2/L)	Color (UC)
Santa Elena locality	6.2187712 N 75.50241516W	Santa Elena creek high part	6.18	1368	<25.0	14.8
San Cristóbal Locality	6.3036804215 75.65491622W	San Cristobal creek "La Iguaná"	6.84	81.3	<25.0	10
Rio Grande reservoir	6.50564438 N 75.53597286W	Rio Grande rersevoir	6.5	52.8	39.6	36.4

Table 4
Recovery of CPF from real samples showing good performance for the Santa Elena and San Cristobal samples, especially at CPF values above 0.5 μg L^{-1}. Rio Grande samples did not show any signal, probably because of the higher organic matter content. n = 3.

Sample	Spiked (μg L^{-1})	Measured by this method (μg L^{-1})	% Recovery (this method)	% RSD	Measured by UHPLC (μg L^{-1})	% Recovery (UHPLC)
Santa Elena locality	0.5	0.06	11.81	4.22	0.36	72
	1	0.84	84.30	3.74	0.7	70
	10	8.83	88.29	2.43	10.05	100.5
San Cristóbal Locality	0,5	0.10	19.72	1.17	0.41	82
	1	1.25	125.13	6.75	0.81	81
	10	10.25	102.53	3.97	8.32	83.2
Rio grande reservoir	0.5	–	–	–	0.37	74.00
	1	–	–	–	0.74	74.00
	10	–	–	–	8.07	80.70

[51].

The findings imply that the fluorescence-based aptasensor can accurately assess >2.85 nM of CPF in superficial waters. However, the use of pretreatments like filtration or the implementation of protective techniques for the ssDNA before using the aptasensor on-site will be a must.

4. Conclusions

A novel fluorescence nanostructured biosensor based on ssDNA aptamer and carbon dots-graphene oxide was developed for the detection of CPF in water. The molecular mechanism of interaction between the aptamer and the target was proposed using bioinformatic tools and a docking energy model, elucidating the specific pocket for the detection in S1 and the most probable residues involved. This modeling gives important insights for system optimization, like the need to apply some aptamer modifications to obtain stronger interaction forces with the pesticide thus increasing the system sensibility. The system works through a FRET mechanism and shows good results for the detection of the pesticide with an exponential relationship of the fluorescence recovery and the pesticide concentration, obtaining a low LOD of 0.01 μg L^{-1}. As it was expected, the specificity of the system is good since other organophosphate pesticides which are usually detected with enzymatic systems, like profenofos, did not show any signal. Moreover, the aptasensor was evaluated for the recovery of CPF in superficial natural water, showing a good performance in the detection of CPF amounts above 2.85 nM in reservoirs with higher conductivity and low amounts of dissolved organic matter. Humic substances usually present in some water sources have been identified as the main interference factor for the on-site use of the proposed aptasensor. To overcome that limitation, a simple pre-treatment step like filtration of the sample could be applied. Considering the low amount of sample, reagents, and the simplicity of the detection process, the practical application of the aptasensor represents a potential advantage to reaching commercial validation, especially when in combination with a portable fluorescent reader.

Regarding the state of the art, the field evaluation, and the explanation about the relationship between water quality and performance is scarce in aptasensors works, so this development is highly valuable for the scientific community. Strategies like the optimization of the aptamer structure generating a truncated alternative, pre-treatment steps, or the protection of the aptamer are crucial for the use of the systems in field assays. However, the proposed system integrates two types of nanomaterials with a novel aptamer technique in a simple way, reaching a lower LOD compared to other high-complex systems. This work paves the way for the implementation of novel systems based on nanotechnology and aptamers for the detection of environmental pollutants.

Funding

This work was supported by the Ministry of Science, Technology, and Innovation of the Colombian government (code 111571451059, contract number FP44842-147-2016).

CRediT authorship contribution statement

María Isabel Gaviria-Arroyave: designed the experiments, conceptualized the paper, perform the conjugation, conducted the detection assays, Formal analysis, wrote the manuscript, in consultation. **Juan Pablo Arango:** perform the conjugation, conducted the detection assays, Formal analysis, wrote the manuscript in consultation. **Kaory Barrientos Urdinola:** perform the conjugation, conducted the detection assays, Formal analysis, wrote the manuscript in consultation. **Juan Bernardo Cano:** Devised and directed the project, wrote the manuscript in consultation. **Gustavo Antonio Peñuela Mesa:** Devised and directed the project, wrote the manuscript in consultation, All authors discussed the results and commented on the manuscript, All authors have read and agreed to the published version of the manuscript.

Declaration of competing interest

The authors declare that they have no known competing financial interests or personal relationships that could have appeared to influence the work reported in this paper.

Data availability

The original contributions presented in the study are included in the article, further inquiries can be directed to the corresponding author

Acknowledgments

The authors would like to thank the Ministry of Science, Technology, and Innovation of the Colombian government for financing the projects “Redes de biosensores aplicados a la detección de contaminantes tóxicos en fuentes naturales que abastecen a las plantas de potabilización” (code 111571451059, contract number FP44842-147-2016). The authors thank the Ministry of Science, Technology, and Innovation of the Colombian government for the scholarship for the doctoral studies of Maria Isabel Gaviria (Grant number 785 of 2017).

References

[1] FAO, PESTICIDES USE. Licencia: CC BY-NC-SA 3.0 IGO, Taken from: https://www.fao.org/faostat/es/#data/RP/visualize, 15/10/2022.
[2] D. Luo, T. Zhou, Y. Tao, Y. Feng, X. Shen, S. Mei, Exposure to organochlorine pesticides and non-Hodgkin lymphoma: a meta-analysis of observational studies, Sci. Rep. 6 (2016) 1–11, https://doi.org/10.1038/srep25768.
[3] S. Mostafalou, M. Abdollahi, The link of organophosphorus pesticides with neurodegenerative and neurodevelopmental diseases based on evidence and mechanisms, Toxicology 409 (2018) 44–52, https://doi.org/10.1016/j.tox.2018.07.014.
[4] J.A. Ramírez, M. Lacasaña, Pesticides: classification, uses, toxicological aspects and exposure assesment, Arch. Prevenvion Riesgos Laborales 4 (2001) 67–75.
[5] M. Liu, A. Khan, Z. Wang, Y. Liu, G. Yang, Y. Deng, N. He, Aptasensors for pesticide detection, Biosens. Bioelectron. 130 (2019) 174–184, https://doi.org/10.1016/j.bios.2019.01.006.

[6] A. Vinotha Alex, A. Mukherjee, Review of recent developments (2018–2020) on acetylcholinesterase inhibition based biosensors for organophosphorus pesticides detection, Microchem. J. 161 (2021), https://doi.org/10.1016/j.microc.2020.105779.

[7] M.I. Gaviria, K. Barrientos, J.P. Arango, J.B. Cano, G.A. Peñuela, Highly sensitive fluorescent biosensor based on Acetylcholinesterase and carbon dots-graphene oxide quenching test for analytical and commercial organophosphate pesticide detection, Front. Environ. Sci. 10 (2022) 1–13, https://doi.org/10.3389/FENVS.2022.825112.

[8] F.F. Talari, A. Bozorg, F. Faridbod, M. Vossoughi, A novel sensitive aptamer-based nanosensor using rGQDs and MWCNTs for rapid detection of diazinon pesticide, J. Environ. Chem. Eng. 9 (2021), 104878, https://doi.org/10.1016/j.jece.2020.104878.

[9] X. Zhu, L. Han, H. Liu, B. Sun, A smartphone-based ratiometric fluorescent sensing system for on-site detection of pyrethroids by using blue-green dual-emission carbon dots, Food Chem. 379 (2022), 132154, https://doi.org/10.1016/j.foodchem.2022.132154.

[10] V. Raveendran, R.N. Kizhakayil, Fluorescent carbon dots as biosensor, green reductant, and biomarker, ACS Omega 6 (2021), 23475, https://doi.org/10.1021/ACSOMEGA.1C03481.

[11] S. Campuzano, P. Yáñez-Sedeño, J.M. Pingarrón, Carbon dots and graphene quantum dots in electrochemical biosensing, Nanomaterials 9 (2019) 1–18, https://doi.org/10.3390/nano9040634.

[12] S. Abdul, R. Nor, M. Zobir, Synthesis, Technology and Applications of Carbon Nanomaterials, Elsevier, Oxford, 2019.

[13] Z.S. Pehlivan, M. Torabfam, H. Kurt, C. Ow-Yang, N. Hildebrandt, M. Yüce, Aptamer and nanomaterial based FRET biosensors: a review on recent advances (2014–2019), Microchim. Acta 186 (2019), https://doi.org/10.1007/s00604-019-3659-3.

[14] M.L. Liu, B. Bin Chen, C.M. Li, C.Z. Huang, Carbon dots: synthesis, formation mechanism, fluorescence origin and sensing applications, Green Chem. 21 (2019) 449–471, https://doi.org/10.1039/c8gc02736f.

[15] K. Phopin, T. Tantimongcolwat, Pesticide aptasensors—state of the art and perspectives, Sensors 20 (2020) 1–40, https://doi.org/10.3390/s20236809.

[16] A. Azzouz, V. Kumar, L. Hejji, K.H. Kim, Advancements in nanomaterial-based aptasensors for the detection of emerging organic pollutants in environmental and biological samples, Biotechnol. Adv. 66 (2023), https://doi.org/10.1016/j.biotechadv.2023.108156.

[17] K. Fan, R. Yang, Y. Zhao, C. Zang, X. Miao, B. Qu, L. Lu, A fluorescent aptasensor for sensitive detection of isocarbophos based on AT-rich three-way junctions DNA templated copper nanoparticles and Fe3O4@GO, Sensor. Actuator. B Chem. 321 (2020), https://doi.org/10.1016/j.snb.2020.128515.

[18] R.V. Nair, P.R. Chandran, A.P. Mohamed, S. Pillai, Sulphur-doped graphene quantum dot based fluorescent turn-on aptasensor for selective and ultrasensitive detection of omethoate, Anal. Chim. Acta 1181 (2021), https://doi.org/10.1016/j.aca.2021.338893.

[19] P. Wang, W. Li, Z. Lu, W. Xiong, K. Zhai, D. Xiang, One-step simultaneous quantitative detection of three pesticides based on bimetallic organic framework nanomaterials and aptamers, Anal. Sci. 38 (2022) 299–305, https://doi.org/10.2116/analsci.21P204.

[20] M.I. Gaviria-Arroyave, J.B. Cano, G.A. Peñuela, Nanomaterial-based fluorescent biosensors for monitoring environmental pollutants: a critical review, Talanta Open 2 (2020), 100006, https://doi.org/10.1016/j.talo.2020.100006.

[21] X. Cheng, Y. Cen, G. Xu, F. Wei, M. Shi, X. Xu, M. Sohail, Q. Hu, Aptamer based fluorometric determination of ATP by exploiting the FRET between carbon dots and graphene oxide, Microchim. Acta 185 (2018) 1–8, https://doi.org/10.1007/s00604-018-2683-z.

[22] R. Oliveira, E. Pinho, A.L. Sousa, Ó. Dias, N.F. Azevedo, C. Almeida, Modelling aptamers with nucleic acid mimics (NAM): from sequence to three-dimensional docking, PLoS One 17 (2022), https://doi.org/10.1371/journal.pone.0264701.

[23] Y. Jiao, W. Hou, J. Fu, Y. Guo, X. Sun, X. Wang, J. Zhao, A nanostructured electrochemical aptasensor for highly sensitive detection of chlorpyrifos, Sensor. Actuator. B Chem. 243 (2017) 1164–1170, https://doi.org/10.1016/j.snb.2016.12.106.

[24] L. ZhaoJing, C. Zhang, L. Yuan, W. Li, H. QiuHui, L. XianJin, Selection of chlorpyrifos-binding ssDNA aptamer by SELEX, Jiangsu J. Agri. Sci. 28 (2012) 198–203.

[25] K. Barrientos, M.I. Gaviria, J.P. Arango, M.E. Londoño, M. Jaramillo, Synthesis, characterization and ecotoxicity evaluation of biochar-derived carbon dots from spruce tree, purple moor-grass and african oil palm, Processes 9 (2021) 16.

[26] M. Zuker, Mfold web server for nucleic acid folding and hybridization prediction..2003, Nucleic Acids Res. 31 (2003) 3406–3415.

[27] J. Stasiewicz, S. Mukherjee, C. Nithin, J.M. Bujnicki, QRNAS: software tool for refinement of nucleic acid structures, BMC Struct. Biol. 19 (2019), https://doi.org/10.1186/s12900-019-0103-1.

[28] National Center for Biotechnology Information, PubChem Compound Summary for CID 2730, 2022. Chlorpyrifos.

[29] I. Tuszynska, M. Magnus, K. Jonak, W. Dawson, J.M. Bujnicki, NPDock: a web server for protein-nucleic acid docking, Nucleic Acids Res. 43 (2015) W425–W430, https://doi.org/10.1093/nar/gkv493.

[30] R. Takahashi, T. Yasuda, Y. Ohmuro-Matsuyama, H. Ueda, BRET Q-body: a ratiometric quench-based bioluminescent immunosensor made of luciferase-dye-antibody fusion with enhanced response, Anal. Chem. 93 (2021) 7571–7578, https://doi.org/10.1021/acs.analchem.0c05217.

[31] M. Yüce, H. Kurt, How to make nanobiosensors: surface modification and characterisation of nanomaterials for biosensing applications, RSC Adv. 7 (2017) 49386–49403, https://doi.org/10.1039/c7ra10479k.

[32] J. Ren, G. Liang, Y. Man, A. Li, X. Jin, Q. Liu, L. Pan, Aptamer-based fluorometric determination of Salmonella Typhimurium using Fe3O4 magnetic separation and CdTe quantum dots, PLoS One 14 (2019), https://doi.org/10.1371/journal.pone.0218325.

[33] T. Tang, J. Deng, M. Zhang, G. Shi, T. Zhou, Quantum dot-DNA aptamer conjugates coupled with capillary electrophoresis: a universal strategy for ratiometric detection of organophosphorus pesticides, Talanta 146 (2016) 55–61, https://doi.org/10.1016/j.talanta.2015.08.023.

[34] P. Singh, S. Kumar, S.K. Verma, Development of fluorescent aptasensor for detection of acephate by utilizing graphene oxide platform, Talanta 252 (2023), https://doi.org/10.1016/j.talanta.2022.123843.

[35] M. Dadmehr, S.C. Shahi, M. Malekkiani, B. Korouzhdehi, A. Tavassoli, A stem-loop like aptasensor for sensitive detection of aflatoxin based on graphene oxide/AuNPs nanocomposite platform, Food Chem. 402 (2023), https://doi.org/10.1016/j.foodchem.2022.134212.

[36] A.M. Onaș, C. Dascălu, M.D. Raicopol, L. Pilan, Critical design factors for electrochemical aptasensors based on target-induced conformational changes: the case of small-molecule targets, Biosensors 12 (2022), https://doi.org/10.3390/bios12100816.

[37] H. Zeng, H. Yang, Y. Tang, X. Niu, Y. Wu, Aptamer-enhanced the Ag(I) ion-3,3′,5,5′-tetramethylbenzdine catalytic system as a novel colorimetric biosensor for ultrasensitive and selective detection of paraquat, Spectrochim. Acta Mol. Biomol. Spectrosc. 280 (2022), https://doi.org/10.1016/j.saa.2022.121571.

[38] U.S. Kadam, K.H. Trinh, V. Kumar, K.W. Lee, Y. Cho, M.H.T. Can, H. Lee, Y. Kim, S. Kim, J. Kang, J.Y. Kim, W.S. Chung, J.C. Hong, Identification and structural analysis of novel malathion-specific DNA aptameric sensors designed for food testing, Biomaterials 287 (2022), https://doi.org/10.1016/j.biomaterials.2022.121617.

[39] S. Salentin, S. Schreiber, V.J. Haupt, M.F. Adasme, M. Schroeder, PLIP: fully automated protein-ligand interaction profiler, Nucleic Acids Res. 43 (2015) W443–W447, https://doi.org/10.1093/nar/gkv315.

[40] M. Arvand, A.A. Mirroshandel, Highly-sensitive aptasensor based on fluorescence resonance energy transfer between L-cysteine capped ZnS quantum dots and graphene oxide sheets for the determination of edifenphos fungicide, Biosens. Bioelectron. 96 (2017) 324–331, https://doi.org/10.1016/j.bios.2017.05.028.

[41] H. Li, X. Huang, J. Huang, M. Bai, M. Hu, Y. Guo, X. Sun, Fluorescence assay for detecting four organophosphorus pesticides using fluorescently labeled aptamer, Sensors 22 (2022), https://doi.org/10.3390/s22155712.

[42] Q. Liu, H. Wang, P. Han, X. Feng, Fluorescent aptasensing of chlorpyrifos based on the assembly of cationic conjugated polymer-aggregated gold nanoparticles and luminescent metal–organic frameworks, Analyst 144 (2019) 6025–6032, https://doi.org/10.1039/c9an00943d.

[43] C. Li, G. Zhang, S. Wu, Q. Zhang, Aptamer-based microcantilever-array biosensor for profenofos detection, Anal. Chim. Acta 1020 (2018) 116–122, https://doi.org/10.1016/j.aca.2018.02.072.

[44] C. Zhu, X. Liu, Y. Li, D. Yu, Q. Gao, L. Chen, Dual-ratiometric electrochemical aptasensor based on carbon nanohorns/anthraquinone-2-carboxylic acid/Au nanoparticles for simultaneous detection of malathion and omethoate, Talanta 253 (2023), 123966, https://doi.org/10.1016/j.talanta.2022.123966.

[45] G. Wang, H. Dong, J. Han, M. Zhang, J. Huang, J. Sun, F. Guan, Z. Shen, D. Xu, X. Sun, Y. Guo, S. Zhao, Interference-resistant aptasensor with tetrahedral DNA nanostructure for profenofos detection based on the composites of graphene oxide and polyaniline, Bioelectrochemistry 148 (2022), https://doi.org/10.1016/j.bioelechem.2022.108227.

[46] Z. Zhang, Y. Luan, S. Ru, H. Teng, Y. Li, M. Liu, J. Wang, A novel electrochemical aptasensor for ultrasensitive detection of herbicide prometryn based on its highly specific aptamer and Ag@Au nanoflowers, Talanta (2023), 124838, https://doi.org/10.1016/j.talanta.2023.124838.

[47] J. Huang, F. Yang, L. Geng, X. Chen, G. Wang, J. Han, Y. Guo, X. Sun, G. Marrazza, A novel electrochemical aptasensor based on core–shell nanomaterial labeling for simultaneous detection of acetamiprid and malathion, Food Chem. 429 (2023), https://doi.org/10.1016/j.foodchem.2023.136857.

[48] Z. Shen, D. Xu, G. Wang, L. Geng, R. Xu, G. Wang, Y. Guo, X. Sun, Novel colorimetric aptasensor based on MOF-derived materials and its applications for organophosphorus pesticides determination, J. Hazard Mater. 440 (2022), https://doi.org/10.1016/j.jhazmat.2022.129707.

[49] F. Luo, Y. Tang, J. Zheng, Z. Xie, J. Wang, J. Zhou, Y. Wu, Smartphone-assisted colorimetric aptasensor for rapid detection of carbendazim residue in agriculture products based on the oxidase-mimicking activity of octahedral Ag2O nanoparticles, Talanta 265 (2023), https://doi.org/10.1016/j.talanta.2023.124845.

[50] J. Park, K.A. Yang, Y. Choi, J.K. Choe, Novel ssDNA aptamer-based fluorescence sensor for perfluorooctanoic acid detection in water, Environ. Int. 158 (2022), https://doi.org/10.1016/j.envint.2021.107000.

[51] B. Peng, P. Liao, Y. Jiang, Preferential interactions of surface-bound engineered single stranded DNA with highly aromatic natural organic matter: mechanistic insights and implications for optimizing practical aquatic applications, Water Res. 223 (2022), https://doi.org/10.1016/j.watres.2022.119015.